MIMO-TDD Reciprocity under Hardware Imbalances: Experimental Results

Xiwen JIANG*, Mirsad Čirkić†‡, Florian Kaltenberger*, Erik G. Larsson‡, Luc Deneire§, Raymond Knopp*
* EURECOM, Campus SophiaTech, 06410 Biot, France
† Ericsson, Ericsson Research, 583 30 Linköping, Sweden
‡ Linköping University, Dept. of Electrical Engineering (ISY), 581 83 Linköping, Sweden
§ Université de Nice Sophia Antipolis, Laboratoire I3S - UMR7271, 06903 Sophia Antipolis, France
xiwen.jiang@eurecom.fr, mirsad.cirkic@ericsson.com

***Abstract*—For time division duplexing (TDD) systems, the physical channel in the air is reciprocal for uplink (UL) and downlink (DL) within the channel coherence time. However when the transceivers' radio frequency (RF) hardware is taken into consideration, TDD channel reciprocity no longer holds because of the non-symmetric characteristics of RF transmit and receive chains. Relative calibration has been proposed to compensate this hardware impairment with a multiplicative matrix. In this paper we perform hardware measurements on this calibration matrix which gives a direct insight on the physical phenomenon of TDD transceivers. Especially, we inspect the assumption that this calibration matrix is diagonal, which is widely adopted in literature but has never been verified by experiments. This work can be regarded as an experimental base for TDD calibration or for theoretical analysis of non-perfect channel reciprocity of TDD systems.**

***Index Terms*—MIMO, TDD, channel reciprocity, relative calibration, hardware impairment.**

I. Introduction

Multi-antenna techniques, such as multi-user multiple-input multiple-output (MU-MIMO) systems, can greatly increase the capacity of mobile communications systems [1]. In order to achieve these gains, these systems require channel state information at the transmitter (CSIT). In a frequency division duplexing (FDD) system CSIT can be obtained using feedback, but this approach is not feasible when a large number of antennas are used (in, e.g., massive MIMO [2], [3], [4]) as the channel would be outdated by the time it is measured and fed back.

In a time division duplexing (TDD) system, on the other hand, the physical channel in the air is reciprocal for uplink (UL) and downlink (DL) within the channel coherence time and we can thus acquire CSIT by measuring the UL channel. However, this property is broken by the non-symmetry of the transmit and receive chains, for which reason, various calibration procedures have been proposed. The existing calibration methods can be classified into two families. The first, referred to as absolute calibration [5], uses additional hardware to perform the calibration separately in the transmitter and the receiver whereas the second, named relative calibration, is totally based on signal processing techniques and is more cost efficient. The idea of relative calibration was firstly put forward in [6], where the authors proposed to use multiplicative matrices to compensate the hardware non-symmetry. The authors in [7] compared the performance and complexity for different problem formulations in time and frequency domains whereas [8] introduced a robust calibration algorithm facing the vulnerability of classical methods to frequency offset on both sides. When it comes to Massive MIMO, the authors in [9] relied on the observation that the ambiguity of a multiplicative scalar on the CSIT would not result in different beamforming antenna patterns and proposed a new calibration strategy where the calibration is done within the same antenna array at one side by taking one element as the reference. In [10], the authors extended this method to non-collocated arrays in a distributed MU-MIMO network.

So far, the literature on relative calibration, e.g. [6], [7], [9], assumes no crosstalk between different radio frequency (RF) chains and the antenna mutual coupling effect is ignored. However studies on hardware impairment show that these effects do exit. For the former, the authors in [11] provided a RF crosstalk model for two interacting chains and studied its impact on the MIMO performance whereas for the latter, authors in [12] had an intensive study and showed the relationship between the antenna mutual coupling matrix and its impedance matrix. It is thus doubtful in the research community whether the relative calibration matrix could really be assumed to be diagonal and the performance degradation arising therefrom is unknown. To address this problem, we carry out measurements of the calibration matrix on EURECOM's OpenAirInterface platform [13] and compare the beamforming performance based on different CSIT acquisition methods. We estimate the full matrix, including the RF chain crosstalk and antenna mutual coupling effect, which has never been done before. The real-world experimental results do not only verify the assumption on the calibration matrix structure but also provide a direct insight on various other phenomenon on the transceiver hardware and can thus be a useful experimental support for TDD reciprocity hardware impairment modeling and relevant theoretical analysis.

This work was partly funded by the French Government (National Research Agency, ANR) through the "Investments for the Future" Program #ANR-11-LABX-0031-01 and by the European Union through the Network of Excellence Newcom# (FP7-ICT-318306, http://www.newcom-project.eu/).

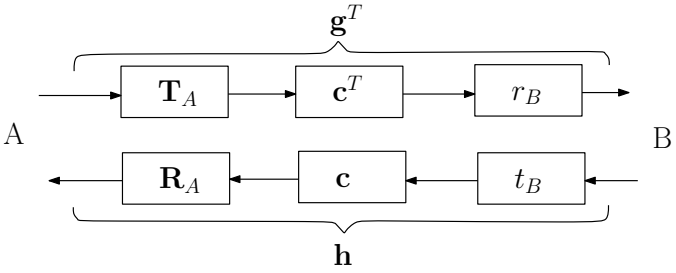

Fig. 1. Reciprocity Model

The rest of the paper is organized as follows: Section II and III present the system model and the outline of relative calibration. In Section IV, we describe the measurement setup and the experimental results. We then perform beamforming based on different CSIT acquisition methods and compare the performance in Section V. Conclusion and future work are pointed out in Section VI.

II. System Model

In our work, we consider a $N \times 1$ multiple-input single-output (MISO) system as illustrated in Fig. 1. Node A is equipped with N antennas and node B has a single antenna. Since the hardware's system characteristics change much slower than the physical channel in the air, they are modeled by linear time invariant (LTI) systems. We note $\boldsymbol{T}_A$ (matrix of size $N \times N$) as the system function in the frequency domain of the transmit block at Node A from the digital-to-analog converter (DAC) to the antenna array. The diagonal elements represent the gains on each transmit chain whereas the off-diagonal elements correspond to the RF chain on-chip crosstalk and the antenna mutual coupling. $\boldsymbol{R}_A$ is the system function of the receive block at node A and includes the characteristics from the antenna array to the analog-to-digital converter (ADC). t_B and r_B represent the transmit and receive chains at node B respectively. The physical channel in the air is assumed to be fully reciprocal, and is noted by $\boldsymbol{c}$. The entire channel seen from the point of view of digital signal processing is composed of the hardware blocks on the transceivers and the physical channel in the air. The forward and reverse links between A and B, represented by $\boldsymbol{g}^T$ and $\boldsymbol{h}$, can thus be modeled as

$$\begin{cases} \boldsymbol{g}^T = r_B \boldsymbol{c}^T \boldsymbol{T}_A \\ \boldsymbol{h} = \boldsymbol{R}_A \boldsymbol{c} t_B. \end{cases} \tag{1}$$

The relationship between these 2 channels is given by

$$\boldsymbol{g}^T = r_B (\boldsymbol{R}_A^{-1} \boldsymbol{h} t_B^{-1})^T \boldsymbol{T}_A = \boldsymbol{h}^T \frac{r_B}{t_B} \boldsymbol{R}_A^{-T} \boldsymbol{T}_A = \boldsymbol{h}^T \boldsymbol{F}, \tag{2}$$

where $\boldsymbol{F} = \frac{r_B}{t_B} \boldsymbol{R}_A^{-T} \boldsymbol{T}_A$ includes all the hardware properties on both sides and is called the calibration matrix.

III. Relative calibration

A TDD system can be designed to work in two phases. During the initialization phase, alternating transmission of the pilots are carried out between two nodes in different time slots within the channel coherence time and the calibration matrix $\boldsymbol{F}$ is estimated based on bidirectional channel estimations. During the transmission phase we can apply (2) to obtain the channel response from A to B using channel estimation from B to A. In this section, we describe how the calibration matrix is estimated during the initialization phase.

Let us consider an orthogonal frequency-division multiplexing (OFDM) system where for each subcarrier the channel can be regarded as flat fading. The signal model is given by

$$\begin{cases} y_b = \boldsymbol{g}^T \boldsymbol{s}_a + n_b \\ \boldsymbol{y}_a = \boldsymbol{h} s_b + \boldsymbol{n}_a, \end{cases} \tag{3}$$

where $y_b \in \mathbb{C}$ and $\boldsymbol{y}_a \in \mathbb{C}^N$ are received signals at node B and node A respectively. $\boldsymbol{s}_a \in \mathbb{C}^N$ and $s_b \in \mathbb{C}$ are the known transmit pilots whereas the noise n_a and $\boldsymbol{n}_b$ are circularly-symmetric complex Gaussian random variables following $\mathcal{CN}(0, \sigma_n^2)$ and $\mathcal{CN}(0, \sigma_n^2 \boldsymbol{I})$ respectively.

The channels can be estimated using received pilots. We adopt here the least square (LS) estimators as they do not require any statistical channel information, given by

$$\begin{cases} \hat{\boldsymbol{g}}^T = y_b \boldsymbol{s}_a^H \left(\boldsymbol{s}_a \boldsymbol{s}_a^H \right)^{-1} \\ \hat{\boldsymbol{h}} = \boldsymbol{y}_a \frac{s_b^*}{\|s_b\|^2}. \end{cases} \tag{4}$$

Since LS estimators are linear, the estimation errors remain circular-symmetric Gaussian variables [14] and follow $\mathcal{CN}\left(0, \sigma_n^2 (\boldsymbol{s}_a^* \boldsymbol{s}_a^T)^{-1}\right)$ and $\mathcal{CN}\left(0, \frac{\sigma_n^2}{\|s_b\|^2} \boldsymbol{I}\right)$ respectively.

Let us consider K pairs of such estimation vectors organized in matrices $\hat{\boldsymbol{G}} = \left[\hat{\boldsymbol{g}}_1, \hat{\boldsymbol{g}}_2, \ldots, \hat{\boldsymbol{g}}_K\right]^T$ and $\hat{\boldsymbol{H}} = \left[\hat{\boldsymbol{h}}_1, \hat{\boldsymbol{h}}_2, \ldots, \hat{\boldsymbol{h}}_K\right]^T$, where $K > N^2$. The estimation problem of the calibration matrix $\boldsymbol{F}$ can be formulated as a total least square (TLS) problem as in [7] and is given by

$$\begin{aligned} \hat{\boldsymbol{F}} = & \underset{\Delta \boldsymbol{H}, \Delta \boldsymbol{G}, \boldsymbol{F}}{\arg\min} \|\Delta \boldsymbol{H}\|_{\mathrm{F}}^2 + \|\Delta \boldsymbol{G}\|_{\mathrm{F}}^2 \\ \text{s.t. } & \hat{\boldsymbol{G}} + \boldsymbol{\Delta G} = (\hat{\boldsymbol{H}} + \Delta \boldsymbol{H}) \boldsymbol{F}, \end{aligned} \tag{5}$$

where $\boldsymbol{\Delta G}$ and $\boldsymbol{\Delta H}$ are the corrections applied to the these estimated values and $\|\cdot\|_{\mathrm{F}}$ is Frobenius norm.

A classical method for solving the TLS problem is based on singular value decomposition (SVD) [15]. Let $\boldsymbol{D} = \begin{bmatrix} \boldsymbol{H} & \boldsymbol{G} \end{bmatrix}$, the SVD algorithm in complex domain gives

$$\boldsymbol{D} = \boldsymbol{U} \boldsymbol{\Sigma} \boldsymbol{V}^H, \tag{6}$$

where $\boldsymbol{\Sigma} = \mathrm{diag}(\sigma_1, ..., \sigma_{2N})$ is composed of the singular values of $\boldsymbol{D}$ and $\sigma_1 \geq ... \geq \sigma_{2N}$. Write $\boldsymbol{V}$ in a block matrix representation as

$$\boldsymbol{V} = \begin{bmatrix} \boldsymbol{V}_{11} & \boldsymbol{V}_{12} \\ \boldsymbol{V}_{21} & \boldsymbol{V}_{22} \end{bmatrix} \tag{7}$$

with $\boldsymbol{V}_{ij}$ $(i, j = 1, 2)$ being $N \times N$ matrices. The sufficient and necessary condition for the existence of a TLS solution is that $\boldsymbol{V}_{22}$ is non-singular. In addition, if and only if $\sigma_N \neq \sigma_{N+1}$ the solution is unique, which is given by

$$\hat{\boldsymbol{F}}_{opt} = -\boldsymbol{V}_{\boldsymbol{12}} \boldsymbol{V}_{\boldsymbol{22}}^{-1}. \tag{8}$$

If the RF chain crosstalk and the antenna mutual coupling are negligible, the transfer function matrices at node A for both transmission and reception, i.e. $\boldsymbol{T}_A$ and $\boldsymbol{R}_A$, are diagonal, so is the relative calibration matrix $\boldsymbol{F}$. The TLS problem in (5) can then be decomposed to N single-input single-output (SISO) problems and could be solved by SVD independently. Adopting this simplification, we reduce N^2 unkown parameters in $\boldsymbol{F}$ to N diagonal elements. In Section IV the calibration matrix obtained by both full estimation and diagonal estimation are illustrated and then in Section V the results are used in a beamforming transmission and the performance is compared.

IV. Measurement Setup and Experimental Results

We carried out the measurements using EURECOM's open-source hardware and software development platform OpenAirInterface [13]. In this section, we describe in detail the measurement setup and the experimental results.

A. Measurement Setup

The measurements in this paper were carried out using ExpressMIMO2 boards as illustrated in Fig. 2. This board is built around a low-cost Spartan-6 150LXT FPGA with native PCIexpress on the FPGA fabric, which is coupled with 4 high-performance LTE RF ASICs on-board, manufactured by Lime Micro Systems (LMS6002D). The chosen RF technology covers a very large part of the available RF spectrum from 300MHz to 3.8GHz with a programmable bandwidth up to 28 MHz. The board can be used together with OpenAirInterface's software defined radio (SDR) OpenAir4G Modem implementing the 3GPP LTE Rel. 8.6 standard and running in real-time on common x86 Linux machines under the control of the Real-Time Application Interface (RTAI). For the measurements in this paper, we however used the non real-time mode by simply sending and receiving frames. All the measurements were taken indoors in a controlled laboratory environment. Two ExpressMIMO2 boards acting as node A and B respectively were connected with cables for both frame and frequency synchronization. We activated multiple RF chains (2 or 4) at node A whereas only the first RF chain of node B was used. The antennas at node A spaced by a quarter of the wavelength had fixed positions whereas we moved around the antenna of node B to create different channels. In order to make the TLS solution converge, channel measurements for different locations of B are preferred to be uncorrelated, for which reason, we randomly chose 45 different locations for node B in the laboratory. In the experiment, we used an LTE-like OFDM waveform for the transmission. Each OFDM symbol consists of 512 carriers, out of which 300 are filled with random QPSK symbols and the rest are set to zero. An extended cyclic prefix (ECP) of 128 samples is added to each OFDM symbol after the 512-point inverse fast Fourier transform (IFFT). The sampling rate is 7.68MSPS, resulting in an effective bandwidth of 4.5MHz. Ten subframes each with 12 ECP-OFDM symbols compose the TDD OFDM frame, the first half of which is used for the transmission from A to B whereas the second half is dedicated for the reverse transmission. When one antenna of node A is on transmission, other antennas of the same side keep silent so that an orthogonality in the time domain is achieved. On each chosen location of B, 10 such TDD OFDM frames are sent to have a better estimation result of the calibration matrix. The carrier frequency used is 1.9 GHz and the transmission power is of around 10dBm. Both transmit and receive gains on all the RF chains are set to 10dB. The receive noise figure is around 10dB. Depending on the location of B, this gives a signal-to-noise ratio (SNR) of up to 40 dB.

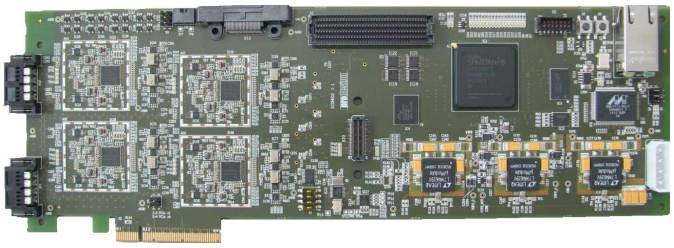

Fig. 2. ExpressMIMO2 board

B. Experimental results

We perform the measurements for 2×1 and 4×1 MISO systems respectively both using full estimation and diagonal estimation and the results are shown by Fig. 3-6 in which each arc is composed of 300 elements covering the whole bandwidth from the first carrier ν_1 to the last carrier ν_{300}. The blue dots are the diagonal elements and other colors are off-diagonal elements both indicated by f_{ij} $(i, j = 1, 2, 3, 4)$ representing the value on the i^{th} row and j^{th} column in $\boldsymbol{F}$. We observe that the diagonal estimations in Figure 4 and 6 are very similar to the corresponding elements in Figure 3 and 5. Diagonal elements are at least 30dB larger than off-diagonal elements. We also observe that the amplitude of diagonal elements have different values between 0.8 and 1.4, which is a result of the RF gain imbalance, knowing that in the perfect case, they should all be 1 under the given configuration. It is also worth noting that the estimation of $\boldsymbol{F}$ is carried out independently for different carriers and the smoothness of the amplitudes over the whole bandwidth implies that efficient pilot design on certain carriers is possible, i.e. in practice, the calibration does not have to be done for all carriers. Moreover, the phases of the elements, taking the first carrier ν_1 as an example, change randomly at each reset of the card, however its evolution as a function of the frequency can be explained by the signal propagation delay on the boards. Let us consider a SISO system model in Fig. 7 where the delay effect is separated from other factors. The delays in blocks t_A, r_A, t_B and r_B are noted by τ_{t_A}, τ_{r_A}, τ_{t_B}, τ_{r_B} respectively and t_{A_0}, r_{A_0}, t_{B_0} and r_{B_0} are blocks without delay. The calibration matrix can be represented as

$$\begin{aligned} f &= \frac{r_B t_A}{t_B r_A} = \frac{r_{B_0} t_{A_0} e^{-j2\pi f \tau_{r_B}} e^{-j2\pi f \tau_{t_A}}}{t_{B_0} r_{A_0} e^{-j2\pi f \tau_{t_B}} e^{-j2\pi f \tau_{r_A}}} \\ &= f_0 e^{-j2\pi f\left[\left(\tau_{t_A}+\tau_{r_B}\right)-\left(\tau_{t_B}+\tau_{r_A}\right)\right]} = f_0 e^{-j2\pi f \Delta\tau} \end{aligned} \tag{9}$$

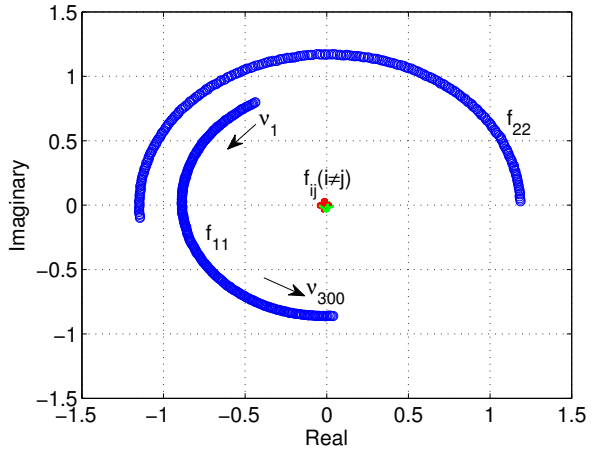

Fig. 3. Full estimation of $\boldsymbol{F}$ in 2×1 MISO

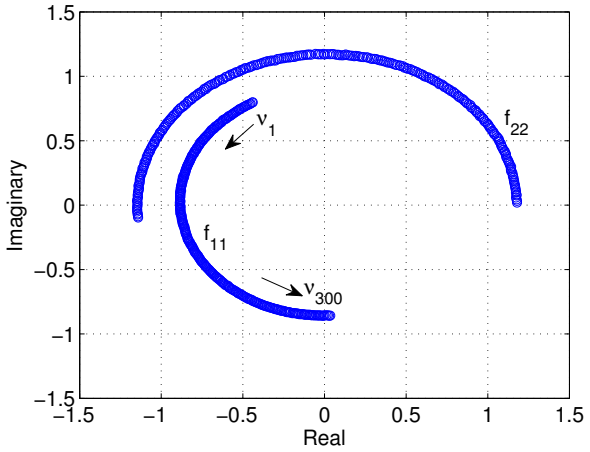

Fig. 4. Diagonal estimation of $\boldsymbol{F}$ in 2×1 MISO

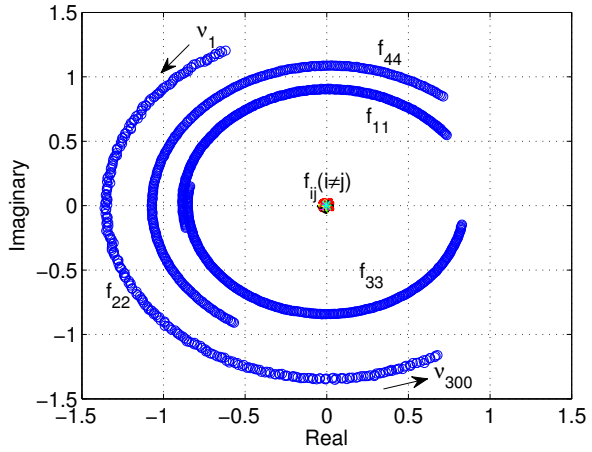

Fig. 5. Full estimation of $\boldsymbol{F}$ in 4×1 MISO

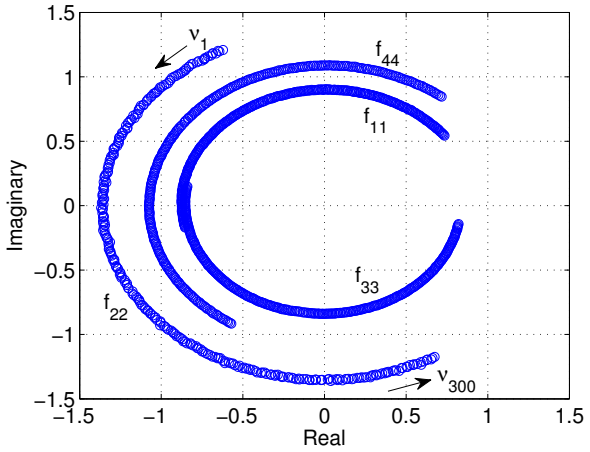

Fig. 6. Diagonal estimation of $\boldsymbol{F}$ in 4×1 MISO

where f_0 is the SISO calibration coefficient without delay and $\Delta\tau = (\tau_{t_A} + \tau_{r_B}) - (\tau_{t_B} + \tau_{r_A})$ is the time delay difference between the transmission from A to B and that from B to A. In our experiment, the total phase spans for different chains over the whole bandwidth are between 0.95π and 1.1π, which correspond to delay differences between $0.1\mu s$ and $0.12\mu s$.

V. Beamforming Performance

When the calibration matrix is obtained in the initializing phase, it can be used in the transmission phase to assess the CSIT using the B to A measurement so that the feedback of the channel information is avoided. In this section we adopt the conjugate beamforming to compare the beamforming performance under different CSIT acquisition methods. Let us consider the signal received by B as

$$y = \boldsymbol{g}^T \boldsymbol{s} + n \tag{10}$$

Conjugate beamforming consists in precoding the transmitted symbol x by the normalized conjugate channel vector as

$$\boldsymbol{s} = \frac{(\hat{\boldsymbol{g}}^T)^H}{\|\hat{\boldsymbol{g}}\|} x = \frac{\hat{\boldsymbol{g}}^*}{\|\hat{\boldsymbol{g}}\|} x \tag{11}$$

We compare the beamforming SNR noted by γ for a randomly chosen location of B under 4 different assumptions.

- Ideal
  In this case, we assume node A knows $\hat{\boldsymbol{g}}$ measured by node B. The beamforming SNR is given by

$$\gamma_{\text{ideal}} = \frac{\|\boldsymbol{g}^T \hat{\boldsymbol{g}}^*\|^2}{\|\hat{\boldsymbol{g}}\|^2} \frac{\sigma_x^2}{\sigma_n^2} \tag{12}$$

- No calibration
  Under this assumption, the transceiver hardware is considered totally reciprocal and $\boldsymbol{h}$ is considered to be equal to $\boldsymbol{g}$, thus no calibration is needed. The SNR is

$$\gamma_{\text{no calib}} = \frac{\|\boldsymbol{g}^T \hat{\boldsymbol{h}}^*\|^2}{\|\hat{\boldsymbol{h}}\|^2} \frac{\sigma_x^2}{\sigma_n^2} \tag{13}$$

- Diagonal $\boldsymbol{F}$ estimation
  The RF chain crosstalk and the antenna mutual coupling are ignored and the calibration matrix is assumed to be diagonal. $\boldsymbol{F}$, noted by $\hat{\boldsymbol{F}}_d$ here, is thus estimated by solving 4 independent SISO TLS problems. The SNR

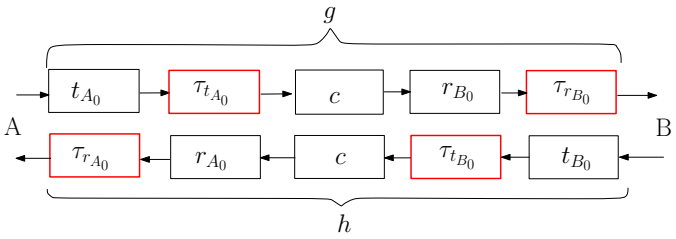

Fig. 7. Reciprocity model with delay

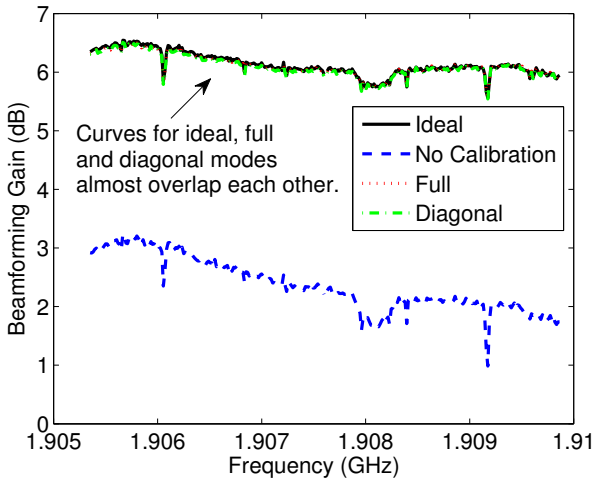

Fig. 8. Beamforming gain of a 4×1 MISO system with regard to a SISO system under different assumptions (SNR averaged over 28 random locations)

is given by

$$\gamma_{\text{diag}} = \frac{\|\boldsymbol{g}^T(\hat{\boldsymbol{h}}^T\hat{\boldsymbol{F}}_d)^H\|^2}{\|\hat{\boldsymbol{h}}^T\hat{\boldsymbol{F}}_d\|^2}\frac{\sigma_x^2}{\sigma_n^2}. \tag{14}$$

- Full $\boldsymbol{F}$ estimation
  Taking into account the RF chain crosstalk and the antenna mutual coupling, we estimate the complete calibration matrix $\boldsymbol{F}$. The SNR is

$$\gamma_{\text{full}} = \frac{\|\boldsymbol{g}^T(\hat{\boldsymbol{h}}^T\hat{\boldsymbol{F}})^H\|^2}{\|\hat{\boldsymbol{h}}^T\hat{\boldsymbol{F}}\|^2}\frac{\sigma_x^2}{\sigma_n^2} \tag{15}$$

We randomly choose 28 new locations for node B in the 4×1 MISO system and let node A transmit data after conjugate precoding under these 4 assumptions. We then spatially average the measured SNR for them and compare with that of a SISO system, where only RF chain 3 in node A is activated, thus obtain the beamforming gain as illustrated in Fig. 8. Note that, this experiment was conducted independently rather than using the data having been collected for the estimation of $\boldsymbol{F}$. We observe that the beamforming gains of both diagonal estimation and full estimation are very similar to that of the ideal case, being around 6dB, which means that the channel reciprocity is fully achieved using relative calibration and ignoring the off-diagonal elements in $\boldsymbol{F}$ is reasonable in a small scale MISO system. When no calibration is used for TDD system, there is some beamforming performance degradation. In our 4×1 MISO system, the average beamforming gain without channel calibration is around 2dB, thus having more than 3dB loss with regard to calibration modes.

VI. Conclusion

In this paper, we presented the calibration experimental setup and the real-world measurement results, which give an insight on the hardware impairment. We also studied the beamforming performance under different CSIT acquisition methods for a small scale MISO system and the results indicate that the diagonal assumption of the calibration matrix in [6], [7] is reasonable. However, when the antenna number scales up, the RF chain crosstalk and the antenna mutual coupling can become more severe as a result of more coupling elements and less antenna spacing due to constrained antenna array size. It is of high interest in the future work to scale up the antenna number of node A to verify whether the calibration matrix can still be assumed to be diagonal in a Massive MIMO case.

References

[1] D. Tse and P. Viswanath, *Fundamentals of wireless communication*. Cambridge university press, 2005.

[2] T. L. Marzetta, "Noncooperative cellular wireless with unlimited numbers of base station antennas," *IEEE Trans. Wireless Commu.*, vol. 9, no. 11, pp. 3590–3600, Nov. 2010.

[3] F. Rusek, D. Persson, B. K. Lau, E. G. Larsson, T. L. Marzetta, O. Edfors, and F. Tufvesson, "Scaling up MIMO: Opportunities and challenges with very large arrays," *IEEE Signal Process. Mag.*, vol. 30, no. 1, pp. 40–60, Jan. 2013.

[4] E. G. Larsson, O. Edfors, F. Tufvesson, and T. L. Marzetta, "Massive MIMO for next generation wireless systems," *IEEE Commun. Mag.*, vol. 52, no. 2, pp. 186–195, Feb. 2014.

[5] A. Bourdoux, B. Come, and N. Khaled, "Non-reciprocal transceivers in ofdm/sdma systems: Impact and mitigation," in *Proc. IEEE Radio and Wireless Conference, (RAWCON)*, Boston, MA, USA, Aug. 2003.

[6] M. Guillaud, D. T. Slock, and R. Knopp, "A practical method for wireless channel reciprocity exploitation through relative calibration," in *Proc. International Symp. Signal Processing and Its Applications (ISSPA)*, Sydney, Australia, Aug. 2005.

[7] F. Kaltenberger, H. Jiang, M. Guillaud, and R. Knopp, "Relative channel reciprocity calibration in MIMO/tdd systems," in *Future Network and Mobile Summit*, Florence, Italy, Jun. 2010.

[8] M. Guillaud and F. Kaltenberger, "Towards practical channel reciprocity exploitation: Relative calibration in the presence of frequency offset," in *IEEE Wireless Communications and Networking Conference (WCNC)*, Shanghai, China, 2013.

[9] C. Shepard, H. Yu, N. Anand, E. Li, T. Marzetta, R. Yang, and L. Zhong, "Argos: Practical many-antenna base stations," in *Proc. ACM International Conf. Mobile computing and networking (Mobicom)*, Istanbul, Turkey, Aug. 2012.

[10] R. Rogalin, O. Bursalioglu, H. Papadopoulos, G. Caire, A. Molisch, A. Michaloliakos, V. Balan, and K. Psounis, "Scalable synchronization and reciprocity calibration for distributed multiuser MIMO," *IEEE Trans. Wireless Commu.*, vol. 13, no. 4, pp. 1815–1831, Apr. 2014.

[11] Y. Jin and F. F. Dai, "Impact of transceiver rfic impairments on MIMO system performance," *IEEE Trans. Ind. Electron.*, vol. 59, no. 1, pp. 538–549, Jan. 2012.

[12] M. Petermann, M. Stefer, F. Ludwig, D. Wübben, M. Schneider, S. Paul, and K.-D. Kammeyer, "Multi-user pre-processing in multi-antenna ofdm tdd systems with non-reciprocal transceivers," *IEEE Trans. Commu.*, vol. 61, no. 9, pp. 3781–3793, Sep. 2013.

[13] N. Nikaein, R. Knopp, F. Kaltenberger, L. Gauthier, C. Bonnet, D. Nussbaum, and R. Ghaddab, "Demo: Openairinterface: An open lte network in a pc," in *Proc. ACM International Conf. Mobile Computing and Networking (MobiCom)*, Maui, Hawaii, USA, 2014.

[14] R. G. Gallager, "Circularly-symmetric gaussian random vectors," *preprint*, 2008.

[15] I. Markovsky and S. Van Huffel, "Overview of total least-squares methods," *Signal processing*, vol. 87, no. 10, pp. 2283–2302, 2007.